

DivCon: Divide and Conquer for Progressive Text-to-Image Generation

Yuhao Jia¹ and Wenhan Tan²

¹ Individual Researcher

² Individual Researcher

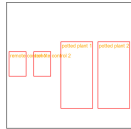
<https://github.com/DivCon-gen/DivCon>

[Numerical Reasoning]

"Two remote controls are sitting on a table next to two potted plants, with their green leaves and vibrant colors adding a cheerful touch to the room."



StableDiffusion (v2.1)



DivCon (Ours) layout + image

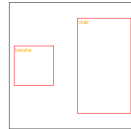


[Spatial Reasoning]

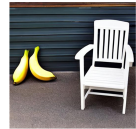
"A banana on the left of a chair."



StableDiffusion (v2.1)



DivCon (Ours) layout + image



"Five handbags and four baseball bats are laid out on a table in a sporting goods store."



StableDiffusion (v2.1)



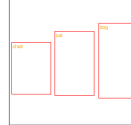
DivCon (Ours) layout + image



"A cat in the middle of chair and dog."



StableDiffusion (v2.1)



DivCon (Ours) layout + image



Fig. 1: Layouts and images generated by our DivCon. DivCon enhances the ability of text-to-image diffusion models to understand complex numerical and spatial relationships in the text.

Abstract. Diffusion-driven text-to-image (T2I) generation has achieved remarkable advancements. To further improve T2I models' capability in numerical and spatial reasoning, the layout is employed as an intermedium to bridge large language models and layout-based diffusion models. However, these methods still struggle with generating images from textural prompts with multiple objects and complicated spatial relationships. To tackle this challenge, we introduce a divide-and-conquer approach which decouples the T2I generation task into simple subtasks. Our approach divides the layout prediction stage into numerical & spatial reasoning and bounding box prediction. Then, the layout-to-image generation stage is conducted in an iterative manner to reconstruct objects from easy ones to difficult ones. We conduct experiments on the HRS and NSR-1K benchmarks and our approach outperforms previous state-of-the-art models with notable margins. In addition, visual results demonstrate that our approach significantly improves the controllability and consistency in generating multiple objects from complex textural prompts.

Keywords: Text-to-Image Generation · Large Language Models · Diffusion Models

1 Introduction

Large-scale text-to-image generation (T2I) models demonstrate exceptional zero-shot capacity in efficiently generating small quantities and varieties of objects [3, 7, 21, 29–31]. However, these methods still suffer from limited capability in generating images from text prompts containing specified object counts, varying sizes, rich details, and complicated spatial relationships [2, 7, 8, 14, 35]. Recently, combining Large Language Models (LLMs) and layout-to-image diffusion models has significantly improved T2I models’ ability in numerical and spatial reasoning [15, 26]. LLMs have strong reasoning and visual planning ability to predict objects’ layouts from the text prompt, which provides more informative conditions for diffusion models to produce higher-quality images.

Despite the significant advancement, existing methods still suffer from limited accuracy when the text prompt contains multiple objects and complicated spatial relationships [2, 26]. Intuitively, the difficulty of synthesizing objects with different characteristics varies a lot. Specifically, LLMs encounter great challenges when conducting simultaneous reasoning and visual planning from complicated text prompts (e.g. "five mice are scurrying around a wooden table, each nibbling on one of the five ripe apples that are laid out on top."). Besides, layout-to-image diffusion models exhibit varying levels of generative proficiency for objects with different sizes, shapes, and details. However, previous methods generate all objects simultaneously without taking their differences into consideration. As a result, objects with higher difficulties cannot be well generated in the images (e.g. toaster and pizza, Fig. 2).

To address this issue, we propose *DivCon*, a training-free approach that applies the *divide-and-conquer* strategy to both layout prediction and image generation phases. Our approach divides complicated tasks into multiple subtasks according to their difficulties and then address these subtasks in an iterative manner. During layout prediction, the number of objects and their spatial relationships are first reasoned from the text prompt. Then, visual planning is performed to predict object bounding boxes. During layout-to-image generation, the diffusion model is first executed to process the layout. Then, the consistency between the synthetic objects and the text prompt is calculated. Next, low-fidelity objects’ layouts are highlighted and fed to the diffusion model to encourage the network to focus on objects with higher difficulties. Extensive experiments have demonstrated that DivCon has significantly improved the quality of generated and achieves state-of-the-art performance on the HRS [2] and NSR-1K [15] benchmark datasets.

Our main contributions can be summarized as follows:

- We propose DivCon, a divide-and-conquer approach for layout-based text-to-image generation by dividing complicated tasks into simple subtasks.



Fig. 2: A comparison of generation difficulty between "toaster" and "pizza". Current methods tend to generate pizza but fail to generate enough toasters or completely miss the category.

- To obtain accurate layouts from the text prompt, we divide the layout prediction stage into numerical & spatial reasoning and bounding box planning.
- To generate high-fidelity images from the layout, we divide layout-to-image generation into two iterations to synthesize objects with different levels of difficulty.
- Experimental results show that our approach achieves significant performance gains, surpassing current state-of-the-art models.

2 Related work

In this section, we review three main categories of text-to-image generation methods: text-to-image generation (T2I) models, layout-conditioned T2I models, and text-to-layout-to-image generation models (Fig. 3).

Text-to-Image (T2I) Generation Models The evolution of large-scale T2I synthesis demonstrates a significant leap forward in the realm of generative models, enabling the creation of detailed and coherent images directly from textual descriptions [3, 17, 21, 29, 31, 38]. Milestone methods in this area are Generative Adversarial Networks (GANs) [21, 32], Variational Autoencoders (VAEs) [6, 12, 29, 38], and diffusion models [3, 19, 25, 28, 31]. GANs often struggle with training stability and mode collapse, whereas VAEs may sometimes produce overly smooth or blurry outputs due to their reconstruction loss. Recently, diffusion models are highly valued for their robustness and ability to generate detailed and realistic images. Particularly, Stable Diffusion [30], which utilizes open vocabulary encoder [27] for encoding text to embeddings as conditional inputs, has demonstrated a remarkable capability for open-world image synthesis, pushing the boundaries of generative models. Despite promising results, a text prompt is usually difficult to provide fine-grained control of the generated images.

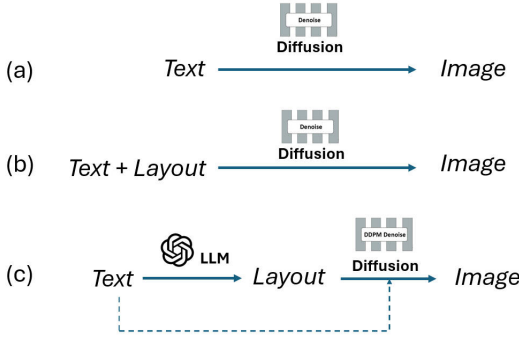


Fig. 3: Three main categories of text-to-image generation methods.

Layout-conditioned T2I Models To improve the controlability of T2I models, prompts like layouts as employed as additional conditions for T2I models. Existing layout-conditioned generation models can be categorized into three branches. One branch of methods trains external networks on layout-images pairs [1, 22, 25, 37, 39]. For instance, GLIGEN incorporates a trainable gated self-attention layer that transforms bounding box information into conditional input for Stable Diffusion. Another branch of methods, including attention-refocusing [26], layout-predictor [34], direct-diffusion [24], layout-guidance [9] and BoxDiff [36], directly manipulate attention maps to optimize the sampling process. These methods generate images with multiple objects through a single forward pass of the diffusion model, resulting in limited fidelity for objects with complicated appearances or spatial relationships. To remedy this, the last branch of methods including Mixture-of-Diffusion [5], MultiDiffusion [4], and LLM-grounded Diffusion [23] perform denoising on each object (*i.e.*, bounding box) separately before fusing the results. However, these methods introduce much higher computational costs. Moreover, the requirements of additional layout prompts hinder their practicality.

Text-to-Layout-to-Image Generation Models Current LLMs have demonstrated strong numerical and spatial reasoning abilities in visual planning and layout generation. Inspired by this, several efforts are made to integrate LLMs to generate layouts from texts, and then utilize layout-conditioned diffusion models for image generation. Attention-refocusing [26] and LLM-grounded Diffusion [23] explore in-context learning of GPT-4 for layout prediction. Layout-GPT [15] searches similar samples from their database as input examples for the LLMs. LLM-layout-generator [10] leverages Chain-of-Thought (CoT) prompting [33] to improve the layout prediction accuracy. However, LLMs are expected to simultaneously perform numerical & spatial reasoning and visual planning of bounding boxes in these methods. Contrary to these methods, we propose a divide-and-conquer approach to conduct reasoning and visual planning separately, which improves the accuracy of layout predictions and substantially

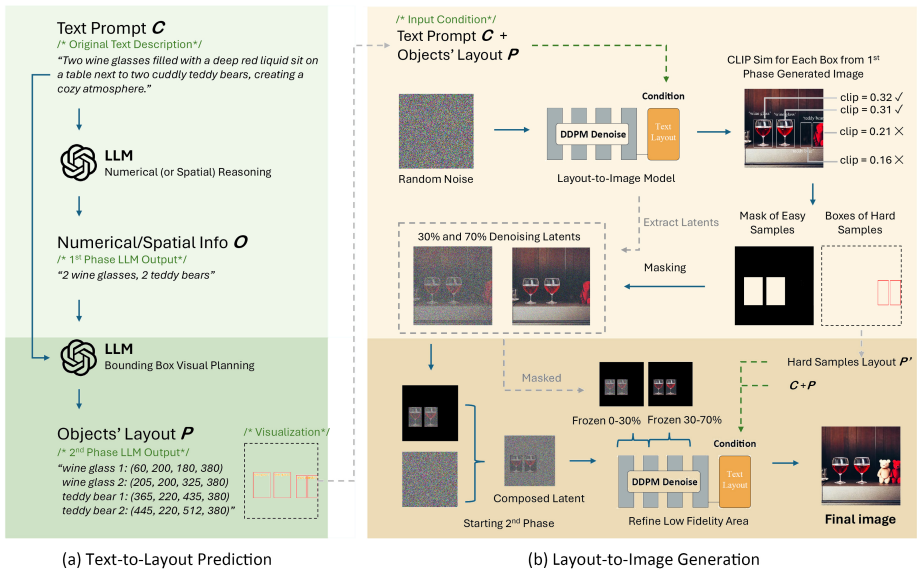


Fig. 4: The proposed DivCon framework. The layout prediction stage is divided into numerical & spatial reasoning and bounding box planning. The layout-to-image generation is divided into two iterations to generate objects with different difficulty levels separately.

advances the prompt fidelity of generated images. In addition, during layout-to-image generation, the objects are synthesized in an iterative manner according to their difficulties, which achieves not only superior fidelity but also significant computational cost savings.

3 Method

3.1 Overview

As illustrated in Fig. 4, our framework comprises two stages. Given a text prompt, LLMs first predict layouts from it. Then, the resultant layout is employed as an additional condition to achieve text-to-image generation. More specifically, each stage is further divided into two steps to handle simple subtasks.

3.2 Text-to-Layout Prediction

Intuitively, to predict the layout from a text prompt, the number & spatial relations of the objects are first required to be reasoned, and then bounding boxes are generated to describe the coordinates & sizes of the objects. However, previous methods commonly conduct these two steps simultaneously without

considering their inherent correlation, thereby hindering them from understanding complicated text prompts well. To remedy this, we introduce the idea of divide-and-conquer to improve the accuracy of predicted layouts. Specifically, leveraging the state-of-the-art large language model GPT-4 [1], numerical and spatial reasoning is first performed, and then bounding boxes are predicted.

Numerical and Spatial Reasoning Given a text prompt C describing an image, an LLM is adopted to predict a set of strings $O = \{s_j | j = 1, 2, \dots, n\}$. If the prompt primarily focused on counting relationships among objects, each string s_j includes both the name and quantity information of each object category j . If the prompt mainly describes spatial relationships, each string s_j will contain the object name and its spatial position in the image. This method allows LLMs to conclude complex numerical and spatial relationships.

Bounding Box Prediction After numerical and spatial reasoning, both the meta prompt C and the prediction result O are fed to the LLM again to predict a list of name-box pairs $P = \{p_i | i = 1, 2, \dots, n\}$. Each pair $p_i = \{o_i : (l_i, t_i, r_i, b_i) | i = 1, 2, \dots, n\}$ consists of the object name o_i and its bounding box’s coordinates (l_i, t_i, r_i, b_i) . The in-context exemplars include a process of correcting the features of generated bounding boxes to ensure the quality of the output layouts.

3.3 Layout-to-Image Generation

After layout prediction, the resultant layout is employed as an additional condition to generate the image. As objects in the layout have different levels of difficulty to synthesize, a divide-and-conquer approach is adopted to reconstruct objects from easy to hard in an iterative manner, as shown in Fig. 4. First, the layout is fed to the diffusion model to synthesize an image. Then, the consistency between the synthetic objects and the text prompt is calculated. Afterward, objects with low fidelity are highlighted and passed to the diffusion model for a second time, encouraging the diffusion model to focus on these difficult objects to achieve higher quality.

First-Round Generation We employ a layout-to-image diffusion model with sampling optimization [26] as the generative model to generate an image conditioned on the text prompt and the predicted layout prompt. During the denoising process, random noise z_T is fed to the diffusion model to gradually denoise it to an image z_0 after T iterations.

Consistency Evaluation With the generated image x , each object is cropped using the bounding boxes in the layout, which are denoted as $x_i \in \mathbb{R}^{4 \times h \times w}$, where $h \times w$ represents the height and width of the bounding box. Then, the CLIP similarity $S_{x_i, o_i} \in (-1, 1)$ is employed to evaluate the consistency between

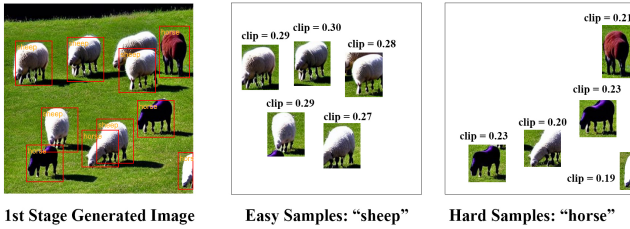


Fig. 5: Comparison of easy and hard samples in a generated image.

the cropped patch and the object name o_i in the text prompt. The higher the similarity is, the higher the fidelity of the corresponding object is. Consequently, the objects with similarities higher than a specified threshold can be considered as easy samples that are "good enough". In contrast, other objects with low similarities are hard samples that are more difficult to reconstruct (e.g. "sheep" and "horse" in Fig. 5). Next, a binary mask M is calculated with bounding boxes of easy objects being set to 1 and the rest regions being set to 0.

Second-Round Refinement After consistency evaluation, different objects are of various levels of fidelity. Our objective is to preserve the "good enough" objects while reproducing the remaining ones to ease the difficulty of diffusion model. To this end, we retrieve the latent representation during the denoising process of the first-round generation. Specifically, $z_{0.7T}$ and $z_{0.3T}$ are first retrieved. Then, the binary mask M is adopted to crop high-fidelity regions in $z_{0.7T}$ and $z_{0.3T}$. Next, the starting noise z'_T for the second-round diffusion is obtained as:

$$z'_T = z_{0.7T} \circ M + \mathcal{N}(\mu, \sigma^2) \circ (1 - M) \quad (1)$$

where \circ is element-wise multiplication and $\mathcal{N}(\mu, \sigma^2)$ is random noise.

The second-round denoising process consists of three stages. First, the input noise z'_T is denoised for $0.3T$ iterations to obtain $z'_{0.3T}$. Second, the high-fidelity regions in $z_{0.7T}$ are cropped and used to replace the corresponding regions in $z'_{0.3T}$ and fed to the diffusion model for another $0.4T$ denoising iterations. Note that, the text prompt and the full layout prompt are employed as conditions in these two stages. Moreover, the regions marked by M is frozen to preserve these high-fidelity regions. During optimization, Cross-Attention Refocusing (CAR) and Self-Attention Refocusing (SAR) losses [26] are employed to update only regions of low fidelity, encouraging the model to focus on these hard samples. Finally, all regions are optimized for the last $0.3T$ iterations to smoothly blend the high-fidelity regions with other regions.

4 Experiments

In this section, we provide an evaluation of our method and compare it with state-of-the-art T2I models. Ablation experiments are conducted to demonstrate the effectiveness of our divide-and-conquer approach in layout prediction and layout-to-image generation stages.

4.1 Experiment Setup

Benchmarks To evaluate the performance of spatial and numerical reasoning in the text-to-image generation tasks, we utilize benchmarks **HRS** [2] and **NSR-1K** [15]. The HRS dataset contains 3,000 prompts (labeled with objects’ names and specific counts) for numerical relationships and 1,002 prompts (labeled with objects’ names and corresponding positions) for spatial relationships. The NSR-1K dataset consists of 762 prompts for numerical relationships and 283 prompts for spatial relationships, all labeled with names, counts, bounding boxes, and ground truth images. We also utilize NSR-1K for quality evaluation. Compared to NSR-1K, HRS exclusively employs natural language prompts, alongside a larger quantity of objects per sample and more intricate spatial relations. This elevates HRS as a more sophisticated and challenging benchmark.

Evaluation Metrics We evaluate the images produced by our methods in terms of both *quality* and *fidelity*.

(1) **Quality** To assess the quality of generated images, we use FID as the metric [18]. Lower FID represents higher similarity between generated images and ground truths images. We report FID in NSR-1K [15] as each prompt has a corresponding ground truth image for FID calculation.

(2) **Fidelity** To evaluate the fidelity of the generated images, grounding accuracy between layouts/images and the text prompt is calculated. Particularly, YOLOv8 [20] is employed to obtain the bounding boxes of the objects in the generated images. In counting, the number of bounding boxes is compared to the ground truths to calculate the precision, recall, F1 score, and accuracy [13, 16]. In spatial relationships, the relative position between two bounding boxes is adopted following PaintSkills [11] and LayoutGPT [15]. Specifically, if the horizontal distance between two bounding boxes exceeds the vertical distance, they are denoted as a left-right relationship. Otherwise, they are denoted as a top-bottom relationship.

Baselines Stable Diffusion [30], Attend-and-Excite [7], and Attention-Refocusing [26] are employed for comparison. Stable Diffusion and Attend-and-Excite directly generate images from the text prompt. Meanwhile, Attention-Refocusing employs layout as an intermedium for image generation.

Table 1: Comparison of our method with baselines on HRS benchmark. Text in bold shows the best results of each metric.

Methods	Numerical								Spatial	
	Layout				Image				LayoutImage	
	Pre.	Rec.	F1	Acc.	Pre.	Rec.	F1	Acc.	Acc.	Acc.
Stable Diffusion 2.1 [30]	-	-	-	-	73.97	53.93	62.38	16.20	-	7.96
Attend-and-Excite [7]	-	-	-	-	76.57	55.94	64.65	18.37	-	9.23
Attention-Refocusing [26]	88.62	91.91	90.44	77.05	77.43	61.78	68.72	25.60	89.57	48.29
DivCon (Ours)	94.17	89.53	91.80	80.73	79.13	63.53	70.48	29.62	91.87	53.87

Table 2: Comparison of our method with baselines on NSR-1K benchmark. Text in bold shows the best results of each metric.

Methods	Numerical								Spatial	
	Layout				Image				LayoutImage	
	Pre.	Rec.	F1	Acc.	Pre.	Rec.	F1	Acc.	Acc.	Acc.
Stable Diffusion 2.1 [30]	-	-	-	-	78.94	75.42	77.41	33.99	-	22.97
Attend-and-Excite [7]	-	-	-	-	79.21	78.62	78.91	39.51	-	29.61
Attention-Refocusing [26]	98.51	99.11	98.81	94.31	84.61	85.64	85.12	56.10	95.05	69.28
DivCon (Ours)	98.47	98.35	98.41	94.39	85.31	87.54	86.41	55.80	96.11	72.95

4.2 Evaluation Results

Quantitative Results We present the results on the HRS benchmark [2] in Tab. 1. As we can see, DivCon outperforms previous T2I models by over 10% in numerical accuracy and over 45% in spatial accuracy, demonstrating its superior numerical and spatial reasoning performance. In addition, DivCon surpasses Attention Refocusing [26] on most metrics. Specifically, our layout prediction improves numerical accuracy by 3% and spatial accuracy by 2%, respectively. For image generation, the F1 score and accuracy achieve 2% and 4% gains, while the spatial accuracy is boosted by up to 6%. By dividing the T2I task into simple subtasks, our DivCon can better understand the text prompt to achieve higher fidelity.

The results on the NSR-1K benchmark are presented in Tab. 2. It can be observed that DivCon outperforms other T2I models by over 15% in numerical accuracy and over 45% in spatial accuracy. As compared to Attention Refocus-

Table 3: FID results achieved by different methods in NSR-1K.

Methods	FID (↓)
Stable Diffusion 2.1 [30]	20.77
Attention-Refocusing [26]	21.05
DivCon (Ours)	20.89

(a) **Prompt:** “Three sandwiches are sitting on a picnic table in a park, while two birds are perched nearby, chirping happily.” (Numerical)



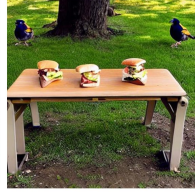
Stable Diffusion



Attend-and-Excite



Attention-Refocusing



DivCon(Ours)

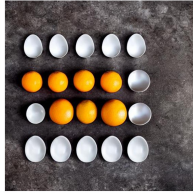
(b) **Prompt:** “There were 5 spoons and 4 oranges on the kitchen counter, glistening in the morning sunlight.” (Numerical)



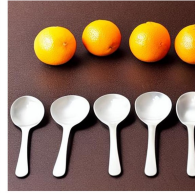
Stable Diffusion



Attend-and-Excite



Attention-Refocusing



DivCon(Ours)

Fig. 6: Qualitative comparison of numerical reasoning between Stable Diffusion, Attend-and-Excite, Attention -Refocusing, and our DivCon.

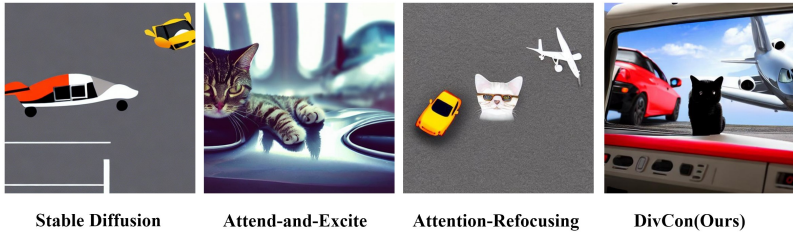
ing [26], our DivCon produces competitive results in terms of layout accuracy. Meanwhile, DivCon achieves approximately 2% superiority in precision, recall, and F1 score for numerical reasoning, and surpasses by nearly 4% in terms of spatial accuracy.

Quantitative results in terms of image quality are shown in Tab. 3. As we can see, our DivCon produces compatible FID scores as compared to stable diffusion and outperforms attention-refocusing with notable margins. This demonstrates that our approach is able to preserve image quality while enhancing prompt fidelity.

Qualitative Results Fig. 6 and Fig. 7 illustrate the qualitative comparison of DivCon and baselines. In all cases, our DivCon can accurately predict the object quantities and the spatial relations from the text prompts.

(1) **Large Quantity of Objects.** Given a prompt containing more than one object category (Fig. 6), Stable Diffusion [30] and Attend-and-Excite [7] often generate an insufficient quantity of objects, while Attention-Refocusing [26] sometimes omits one category of objects or generates an excessive number of objects. For instance, the prompt in Fig. 6(b) contains five spoons and four oranges. However, Stable Diffusion and Attend-and-Excite cannot synthesize sufficient spoons or oranges. Meanwhile, Attention-Refocusing generates an excess number of objects, with spoons appearing incomplete due to missing parts. As compared to these methods, our DivCon achieves superior numerical accuracy.

(a) Prompt: "A cat among car and airplane." (Spatial)



(b) Prompt: "A person and a dog in the middle of horse and banana." (Spatial)



Fig. 7: Qualitative comparison of spatial reasoning between Stable Diffusion, Attend-and-excite, Attention -Refocusing and our DivCon.

(2) **Complicated Spatial Relation.** Given a prompt containing complex spatial relationships among more than two object categories (Fig. 7, previous T2I models struggle to generate correct spatial relations. Meanwhile, Attention-Refocusing tends to produce distortion or blending artifacts around the boundaries of objects. In Fig. 7 (b), Stable Diffusion and Attend-and-Excite miss certain object categories, while Attention-Refocusing merges the color of the banana with the person. In contrast, our DivCon inference accurate object categories and their spatial relationships, exhibiting superior performance in these challenging cases.

4.3 Ablation Study

In this sub-section, we conduct ablation experiments to evaluate the effectiveness of our divide-and-conquer approach in both layout prediction and image generation. Results are presented in Tab. 4 and Attention-Refocusing [26] is used as the baseline.

Divide-and-Conquer in Layout Prediction To demonstrate the effectiveness of our divide-and-conquer approach in the layout prediction stage, we develop a variant by conducting numerical & spatial reasoning and bounding box prediction in a single step. As we can see, our divide-and-conquer approach produces consistent improvements across all metrics, with an increase of 4% in both

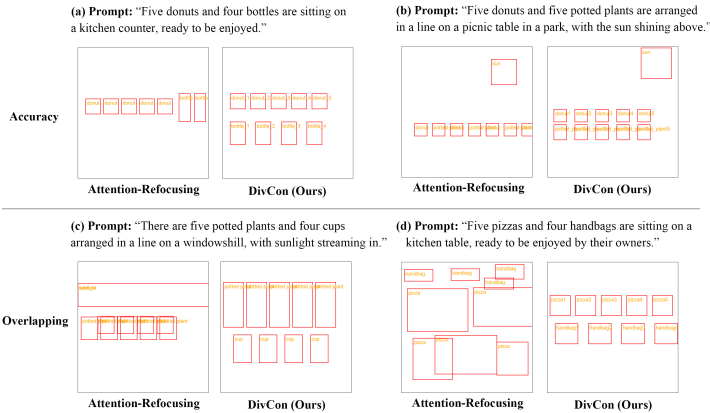


Fig. 8: Comparison of layouts generated from Attention-Refocusing and our DivCon.

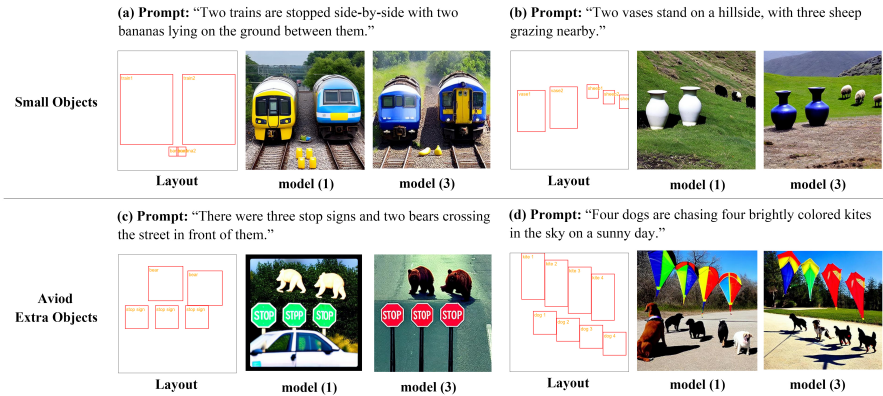


Fig. 9: Ablation study of our image generation.

numerical and spatial accuracy. We further compare the layouts predicted by our DivCon and Attention-Refocusing in Fig. 8. Compared to Attention-Refocusing, layouts generated by our DivCon not only exhibit higher reasoning accuracy (Fig. 8 (a), (b)) but also are more organized with less overlap (Fig. 8 (c), (d)).

Divide-and-Conquer in Image Generation To study the effectiveness of our divide-and-conquer approach in the image generation stage, we develop a variant to synthesize the image in a single forward pass. It can be observed from Tab. 4 that the divide-and-conquer approach facilitates our method to notable performance gains in terms of all metrics. We further compare the results produced by our method using prompts containing multiple objects in Fig. 9. As we can see, the divide-and-conquer approach facilitates our DivCon to better reconstruct the objects, especially for small-sized ones, while avoiding generating

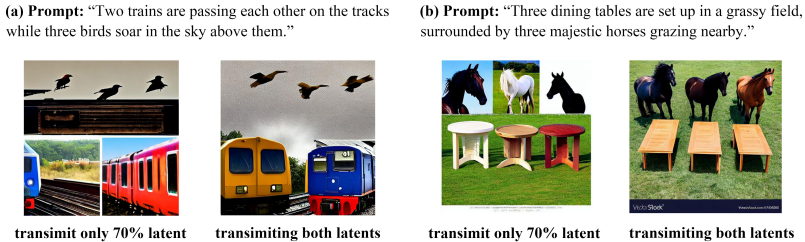


Fig. 10: Comparison of transmit one or two latent representations.

Table 4: Ablation study of our method’s image generation performance on HRS benchmark. "Layout w/DivCon": Layout prediction from LLMs with divide-and-conquer prompting. "Image w/DivCon": Layout-to-Image generation with divide-and-conquer strategy.

	Layout w/DivCon	Image w/DivCon	Numerical				Spatial
			Precision	Recall	F1	Acc.	Acc.
(1)	-	-	77.43	61.78	68.72	25.60	48.29
(2)	✓	-	78.26	62.61	69.57	29.46	52.74
(3)	-	✓	78.18	62.36	69.38	27.83	53.17
(4)	✓	✓	79.13	63.53	70.48	29.62	53.87

objects outside the designated bounding boxes. For example, in Fig. 9(a), DivCon accurately reconstructs the small objects. In Fig. 9(d), DivCon successfully avoids generating the dog outside boxes.

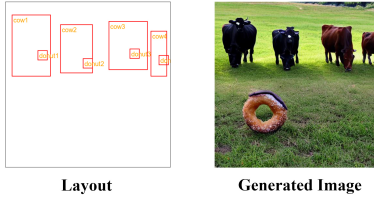
Overall, with our divide-and-conquer approach in both layout prediction and image generation stages, our DivCon produces the best accuracy and surpasses Attention-Refocusing by approximately 2% on numerical f1, 4% on numerical accuracy, and 6% on spatial accuracy.

Fractiles in Image Generation During image generation of our DivCon, two fractiles (*i.e.*, $z_{0.3T}$ and $z_{0.7T}$) are used to preserve “good enough” results in the first-round generation. We conduct ablation experiments to study these two fractiles. The second fractile $z_{0.7T}$ marks the end of optimization and is non-adjustable. We observe that transmitting only $z_{0.7T}$ to the next phase results in instability in image generation instability, specifically manifesting as noticeable boundary demarcations of bounding boxes in the images (Fig. 10).

We further compare the performance achieved by our model with different values for the first fractile. Experiment results are presented in Tab. 5. It can be observed that the model suffers a notable performance drop if only the second fractile is employed. With an additional fractile, our DivCon yields a notable improvement. Additionally, the selection of the first fractile’s value exhibits a marginal impact on the efficacy of the model, with the 30% threshold demonstrating optimal performance.

Table 5: Ablation study of two fractiles used to preserve results in the first-round generation.

First Fractile	Second Fractile	Numerical				Spatial
		Precision	Recall	F1	Acc.	Acc.
-	✓	76.82	60.69	67.80	24.31	48.53
0.1 T	✓	78.44	61.61	69.01	29.12	52.30
0.3 T	✓	79.13	63.53	70.48	29.62	53.87
0.5 T	✓	78.13	63.25	69.90	28.71	51.46

(a) Prompt: "Four cows are happily munching on four donuts in a grassy field."**Fig. 11:** Comparison of transmit one or two latent representations.

5 Limitations and Discussions

As illustrated in Fig. 11, our method still struggles with generating objects from certain pattern layouts. When the text prompt describes objects overlapping in space, the diffusion model may fail to generate all objects accurately. This limitation stems from the inherent capacity of layout-conditioned image generation models to handle overlapping boxes. Despite these challenges, our approach still demonstrates a reduced frequency of overlapping in layout prediction compared to the base model.

6 Conclusion

In this work, we introduce DivCon, a novel divide-and-conquer approach that divides the text-to-image generation task into simple subtasks to achieve higher image generation fidelity. Specifically, the layout prediction is divided into two steps to conduct numerical & spatial reasoning and bounding box prediction, respectively. Then, layout-to-image generation is achieved via an iterative manner to synthesize objects in an easy-to-hard fashion. Comprehensive experiments demonstrate that our DivCon outperforms existing state-of-the-art grounded text-to-image models in terms of both image quality and prompt fidelity.

References

1. Avrahami, O., Hayes, T., Gafni, O., Gupta, S., Taigman, Y., Parikh, D., Lischinski, D., Fried, O., Yin, X.: Spatext: Spatio-textual representation for controllable image generation. In: CVPR (2023) [4](#)
2. Bakr, E.M., Sun, P., Shen, X., Khan, F.F., Li, L.E., Elhoseiny, M.: Hrs-bench: Holistic, reliable and scalable benchmark for text-to-image models. In: ICCV. pp. 20041–20053 (2023) [2](#), [8](#), [9](#)
3. Balaji, Y., Nah, S., Huang, X., Vahdat, A., Song, J., Zhang, Q., Kreis, K., Aittala, M., Aila, T., Laine, S., Catanzaro, B., Karras, T., Liu, M.Y.: ediff-i: Text-to-image diffusion models with an ensemble of expert denoisers. arXiv preprint arXiv:2211.01324 (2022) [2](#), [3](#)
4. Bar-Tal, O., Yariv, L., Lipman, Y., Dekel, T.: Multidiffusion: Fusing diffusion paths for controlled image generation (2023) [4](#)
5. Álvaro Barbero Jiménez: Mixture of diffusers for scene composition and high-resolution image generation. arXiv preprint arXiv:2302.02412 (2023) [4](#)
6. Chang, H., Zhang, H., Barber, J., Maschinot, A., Lezama, J., Jiang, L., Yang, M.H., Murphy, K., Freeman, W.T., Rubinstein, M., Yuanzhen, L., Dilip, K.: Muse: Text-to-image generation via masked generative transformers. arXiv preprint arXiv:2301.00704 (2023) [3](#)
7. Chefer, H., Alaluf, Y., Vinker, Y., Wolf, L., Cohen-Or, D.: Attend-and-excite: Attention-based semantic guidance for text-to-image diffusion models. ACM Transactions on Graphics (TOG) **42**(4), 1–10 (2023) [2](#), [8](#), [9](#), [10](#)
8. Chen, M., Laina, I., Vedaldi, A.: Training-free layout control with cross-attention guidance. arXiv preprint arXiv:2304.03373 (2023) [2](#)
9. Chen, M., Laina, I., Vedaldi, A.: Training-free layout control with cross-attention guidance. arXiv preprint arXiv:2304.03373 (2023) [4](#)
10. Chen, X., Liu, Y., Yang, Y., Yuan, J., You, Q., Liu, L.P., Yang, H.: Reason out your layout: Evoking the layout master from large language models for text-to-image synthesis. arXiv preprint arXiv:2311.17126 (2023) [4](#)
11. Cho, J., Zala, A., Bansal, M.: Dall-eval: Probing the reasoning skills and social biases of text-to-image generative transformers. arXiv preprint arXiv:2202.04053 (2022) [8](#)
12. Ding, M., Zheng, W., Hong, W., Tang, J.: Cogview2: Faster and better text-to-image generation via hierarchical transformers. arXiv preprint arXiv:2204.14217 (2022) [3](#)
13. El-Nouby, A., Sharma, S., Schulz, H., Hjelm, D., El Asri, L., Ebrahimi Kahou, S., Bengio, Y., Taylor, G.W.: Tell, draw, and repeat: Generating and modifying images based on continual linguistic instruction. In: ICCV (2019) [8](#)
14. Feng, W., He, X., Fu, T.J., Jampani, V., Akula, A., Narayana, P., Basu, S., Wang, X.E., Wang, W.Y.: Training-free structured diffusion guidance for compositional text-to-image synthesis. In: ICLR (2023) [2](#)
15. Feng, W., Zhu, W., jui Fu, T., Jampani, V., Akula, A., He, X., Basu, S., Wang, X.E., Wang, W.Y.: Layoutgpt: Compositional visual planning and generation with large language models. In: NeurIPS (2023) [2](#), [4](#), [8](#)
16. Fu, T.J., Wang, X.E., Grafton, S., Eckstein, M., Wang, W.Y.: Sscr: Iterative language-based image editing via self-supervised counterfactual reasoning. In: Conference on Empirical Methods in Natural Language Processing (EMNLP) (2020) [8](#)

17. Gafni, O., Polyak, A., Ashual, O., Sheynin, S., Parikh, D., Taigman, Y.: Make-a-scene: Scene-based text-to-image generation with human priors. In: ECCV. pp. 89–106. Springer (2022) [3](#)
18. Heusel, M., Ramsauer, H., Unterthiner, T., Nessler, B., Hochreiter, S.: Gans trained by a two time-scale update rule converge to a local nash equilibrium. In: NeurIPS. vol. 30 (2017) [8](#)
19. Ho, J., Jain, A., Abbeel, P.: Denoising diffusion probabilistic models. In: NeurIPS. pp. 6840–6851 (2020) [3](#)
20. Jocher, G., Chaurasia, A., Qiu, J.: Ultralytics YOLO (Jan 2023), <https://github.com/ultralytics/ultralytics> [8](#)
21. Kang, M., Zhu, J.Y., Zhang, R., Park, J., Shechtman, E., Paris, S., Park., T.: Scaling up gans for text-to-image synthesis. In: CVPR. pp. 10124–10134 (2023) [2](#), [3](#)
22. Li, Y., Liu, H., Wu, Q., Mu, F., Yang, J., Gao, J., Li, C., Lee, Y.J.: Gligen: Open-set grounded text-to-image generation. In: CVPR (2023) [4](#)
23. Lian, L., Li, B., Yala, A., Darrell, T.: Llm-grounded diffusion: Enhancing prompt understanding of text-to-image diffusion models with large language models. arXiv preprint arXiv:2305.13655 (2023) [4](#)
24. Ma, W.D.K., Lewis, J., Kleijn, W.B., Leung, T.: Directed diffusion: Direct control of object placement through attention guidance. arXiv preprint arXiv:2302.13153 (2023) [4](#)
25. Nichol, A.Q., Dhariwal, P., Ramesh, A., Shyam, P., Mishkin, P., Mcgrew, B., Sutskever, I., Chen, M.: GLIDE: Towards photorealistic image generation and editing with text-guided diffusion models. In: ICML. pp. 16784–16804. PMLR (2022) [3](#), [4](#)
26. Phung, Q., Ge, S., Huang, J.B.: Grounded text-to-image synthesis with attention refocusing. arXiv preprint arXiv:1905.00538 (2023) [2](#), [4](#), [6](#), [7](#), [8](#), [9](#), [10](#), [11](#)
27. Radford, A., Kim, J.W., Hallacy, C., Ramesh, A., Goh, G., Agarwal, S., Sastry, G., Askell, A., Mishkin, P., Clark, J., Krueger, G., Sutskever, I.: Learning transferable visual models from natural language supervision. In: ICML. pp. 8748–8763. PMLR (2021) [3](#)
28. Ramesh, A., Dhariwal, P., Nichol, A., Chu, C., Chen, M.: Hierarchical text-conditional image generation with clip latents. arXiv preprint arXiv:2204.06125 (2022) [3](#)
29. Ramesh, A., Pavlov, M., Goh, G., Gray, S., Voss, C., Radford, A., Chen, M., Sutskever, I.: Zero-shot text-to-image generation. In: ICML. pp. 8821–8831. PMLR (2021) [2](#), [3](#)
30. Rombach, R., Blattmann, A., Lorenz, D., Esser, P., Ommer, B.: High-resolution image synthesis with latent diffusion models. In: CVPR. pp. 10684–10695 (2022) [2](#), [3](#), [8](#), [9](#), [10](#)
31. Saharia, C., Chan, W., Saxena, S., Li, L., Whang, J., Denton, E., Ghasemipour, S.K.S., Ayan, B.K., Mahdavi, S.S., Lopes, R.G., Salimans, T., Ho, J., Fleet, D.J., Norouzi, M.: Photorealistic text-to-image diffusion models with deep language understanding. In: NeurIPS. vol. 35, pp. 36479–36494 (2022) [2](#), [3](#)
32. Sauer, A., Karras, T., Laine, S., Geiger, A., Aila, T.: Stylegan-t: Unlocking the power of gans for fast large-scale text-to-image synthesis. arXiv preprint arXiv:2301.09515 (2023) [3](#)
33. Wei, J., Wang, X., Schuurmans, D., Bosma, M., Xia, F., Chi, E., Le, Q.V., Zhou, D., et al.: Chain-of-thought prompting elicits reasoning in large language models. In: NeurIPS. vol. 35, pp. 24824–24837 (2022) [4](#)

34. Wu, Q., Liu, Y., Zhao, H., Bui, T., Lin, Z., Zhang, Y., Chang, S.: Harnessing the spatial-temporal attention of diffusion models for high-fidelity text-to-image synthesis. arXiv preprint arXiv:2304.03869 (2023) [4](#)
35. Xiao, G., Yin, T., Freeman, W.T., Durand, F., Han, S.: Fastcomposer: Tuning-free multi-subject image generation with localized attention. arXiv preprint arXiv:2305.10431 (2023) [2](#)
36. Xie, J., Li, Y., Huang, Y., Liu, H., Zhang, W., Zheng, Y., Shou, M.Z.: Boxdiff: Text-to-image synthesis with training-free box-constrained diffusion. arXiv preprint arXiv:2307.10816 (2023) [4](#)
37. Yang, Z., Wang, J., Gan, Z., Li, L., Lin, K., Wu, C., Duan, N., Liu, Z., Liu, C., Zeng, M., et al.: Reco: Region-controlled text-to-image generation. arXiv preprint arXiv:2211.15518 (2022) [4](#)
38. Yu, J., Xu, Y., Koh, J.Y., Luong, T., Baid, G., Wang, Z., Vasudevan, V., Ku, A., Yang, Y., Ayan, B.K., Hutchinson, B., Wei, H., Parekh, Z., Li, X., Zhang, H., Baldrige, J., Wu, Y.: Scaling autoregressive models for content-rich text-to-image generation. Transactions on Machine Learning Research (2022) [3](#)
39. Zhang, L., Rao, A., Agrawala, M.: Adding conditional control to text-to-image diffusion models. In: ICCV. pp. 3836–3847 (2023) [4](#)